Title

SEISMIC PERFORMANCE OF STONE MASONRY BUILDINGS USED IN THE HIMALAYAN BELT

Authors

Qaisar Ali, Akhtar Naeem Khan, Mohammad Ashraf, Awais Ahmed, Bashir Alam, Naveed Ahmad, Mohammad Javed, Shahzad Rahman, Mohammad Fahim, Mohammad Umar

Corresponding (first) author: Qaisar Ali

Mailing address: Earthquake Engineering Center at Civil Engineering Department
University of Engineering and Technology
Peshawar
Pakistan

Phone: +92-91-919218569

Fax: +92-91-9218223

E-mail address: **drqaisarali@nwfpuet.edu.pk**

SEISMIC PERFORMANCE OF STONE MASONRY BUILDINGS USED IN THE HIMALAYAN BELT

Qaisar Ali[1], Akhtar Naeem Khan[1], Mohammad Ashraf[1], Awais Ahmed[1], Bashir Alam[1], Naveed Ahmad[1], Mohammad Javed[1], Shahzad Rahman[1], Mohammad Fahim[1], Mohammad Umar[1]

Rubble-stone masonry structures are abundantly found in the Asian countries along the Himalayan range. Such structures are usually constructed in dry-stone masonry, or are constructed in mud mortar, which makes them susceptible to damage and collapse in earthquakes. In order to study the seismic behavior of these structures, dynamic shake table tests on three reduced scale rubble-stone masonry models were conducted. The models comprised a representative school building, a residential building and a model incorporating simple cost-effective features in the form of horizontal and vertical reinforced concrete elements. This paper presents the results of shake table tests carried out on rubble-stone masonry buildings including: damage pattern, capacity curves, damage limit states and response modification factors of these structures. Test data indicates that seismic performance of rubble-stone masonry structures can be significantly improved by incorporating cost-effective features such as vertical members and relatively thin horizontal bands.

INTRODUCTION

Stone masonry buildings constitute a substantial portion of the total building stock of the areas of Asian countries such as, Afghanistan, Pakistan, India, Nepal and Bhutan, which fall in the Himalayan belt. Based on the combination of different systems of walls, roof and floors, a variety of stone masonry buildings exist in these countries. The main construction techniques and structural features of these buildings are however fairly uniform throughout the Himalayan belt, even though the area is inhabited by people from different cultures and civilizations.

[1] Earthquake Engineering Center, Department of Civil Engineering, University of Engineering and Technology Peshawar, Pakistan

The most common construction type in these areas consist of two wythes random-rubble-stone masonry walls in dry or mud mortar as shown in figure 1, with flat earthen or pitched galvanized iron sheet roof. The seismic performance of these buildings in the past earthquakes has been considered to be quite poor (EERI, World Housing Encyclopedia, 2008). Such buildings are therefore believed as one of the most seismically vulnerable structures. Collapse of such structures featured prominently in the Kashmir Earthquake of October 08, 2005 that left about 80,000 people dead and around 3.5 million homeless (Ali. Q et al. 2005; Naseer et al., 2010).

Since stone is an abundant and easily available construction material compared to burnt clay bricks and concrete in these areas, stone masonry buildings are bound to remain natural choice of the general populace of these areas for the foreseeable future. Moreover, under the prevailing economic conditions of these areas, the chances of replacing stone by an alternate building material are low.

Different experts and agencies over the years have recommended a number of strengthening features to improve the seismic performance of stone masonry buildings (IAEE 1986; IS 13828 1993 and Tomazevic M 1999), the most common recommended and adopted features consist of provision of horizontal bands and/or vertical elements made of Reinforced Concrete (RC) or timber. These recommendations, by and large, are based on intuition, lessons learned from the past earthquakes, engineering judgment and/or limited research results derived from studying similar structures. A classic example of the use of horizontal and vertical timber elements for improving seismic performance of stone masonry buildings from one of the remote northern areas of Pakistan, Gilgit, is shown in figure 2. History has shown that these features significantly improve the seismic performance of conventional random-rubble-stone masonry buildings (Ali Q and Muhammad T 2006). The scientific quantification of the performance of these structures is however still lacking.

There exist enough experimental and numerical studies on seismic performance of buildings made from unreinforced brick, block and dressed stone masonry (Gulkan P.et.al 1979 ; Mann W 1982; Calvi G M 1996 ; Tomazevic M 1999 ; Ali Q and Naeem A 2007), however, studies on random rubble-stone masonry in dry masonry construction or using mud mortar are quite limited (G. Vasconcelos et.al. 2006).

The present investigation discusses the results of three shake table tests conducted on rubble-stone masonry structures found in abundance in the Northern Areas of Pakistan and in the rest of the Himalayan belt. The three models tested comprised the following:

1. A representative school building:
2. A residential building:
3. A model incorporating simple cost effective seismic features in the form of horizontal and vertical reinforced concrete elements.

All of the models were constructed on reduced scale of 1:3 and were subjected to actual acceleration records from past earthquakes. The paper presents test results including: damage pattern, capacity curves, damage limit states and response modification factors of these structures. The test data indicates that seismic performance of rubble-stone masonry structures can be significantly improved by incorporating low-cost modifications.

DESCRIPTION OF TESTED MODELS

Reduced scale stone masonry models are named SM1, SM2 and SM3. All the tested models were single story with a single room. The size of all models was 1500 mm x 1200 mm according to a scale factor of 3 for a prototype size of 4500 mm x 3600 mm. The thickness of the walls of model SM1 was 150 mm and that of models SM2 and SM3 was 125 mm corresponding to prototype wall thicknesses of 450 mm and 375 mm respectively. The walls of the models were named as W1, W2, W3 and W4. In each case, walls W1 and W3 were the long walls having door and window openings whereas W2 and W4 were the solid short walls. Since the strength of stones and mud mortar could not be reduced, simple model similitude principles as given in table 1 were followed in the reduced scale modeling.

The attributes of model SM1 were set to represent the construction type of typical public buildings, especially schools and basic healthcare units used in the highly seismic Northern areas of Pakistan. Statistics show that about 18000 school children died as a result of partial or total collapse of 7669 schools, mostly consisting of SM1-type stone masonry buildings, in the Kashmir Earthquake of October 08, 2005 (Asian Development Bank & World Bank 2005). These buildings were typically constructed in 450 mm thick, two wythes Coursed Random Rubble (CRR) walls using half dressed stones placed in cement sand mortar without vertical

elements and/ or horizontal bands except roof band. The stones are dressed on the bed and outer sides but all the other sides remain undressed. The roof in most cases was Reinforced Concrete (RC) slab. Model SM1 was therefore constructed to contain most of the characteristics of such school buildings in order to investigate their seismic performance. Table 2 shows the characteristics of the prototype and the scaled model SM1 and figure 3 shows the construction details of the model.

Table 1. Similitude requirement for simple model

Physical Quantity	Relationship	Scale factor
Length (L)	$S_L = L_P/L_M$	3.00
Stress, Strength (f)	$S_f = f_P/f_M$	1.00
Strain (ε)	$S_\varepsilon = \varepsilon_P/\varepsilon_M$	1.00
Specific Mass (ρ)	$S_\rho = \rho_P/\rho_M$	1.00
Displacement (d)	$S_d = d_P/d_M = S_L$	3.00
Force (F)	$S_F = F_P/F_M = S_L^2 S_f$	9.00
Time (t)	$S_t = t_P/t_M = S_L\sqrt{(S_\varepsilon S_\rho/S_f)}$	3.00
Frequency (Ω)	$S_\Omega = \Omega_P/\Omega_M = 1/S_t$	0.33
Velocity (v)	$S_v = v_P/v_M = \sqrt{(S_\varepsilon S_\rho/S_f)}$	1.00
Acceleration (a)	$Sa = a_P/a_M = S_f/(S_L S_\rho)$	0.33

Table 2. Model SM1 parameters

Parameter	SM1	
	Prototype	**Model**
Stone masonry walls	450 mm thick coursed random rubble	150 mm thick coursed random rubble
Stones	Half Dressed	Half Dressed
Mortar	Cement sand mortar having compressive strength of 4.0 MPa	Cement sand mortar having compressive strength of 4.0 MPa
Concrete	Concrete having compressive strength of 17.0 MPa	Concrete having compressive strength of 17.0 MPa
Reinforcement	Mild steel having yield strength of 280 MPa	Mild steel having yield strength of 280 MPa
Vertical elements	No vertical elements	No vertical elements

Horizontal bands	Continuous roof band; 150 mm thick horizontal band reinforced with 4, 10.0 mm longitudinal bars and 3.0 mm stirrups @ 150 mm centre to centre	Continuous roof band; 50 mm thick horizontal band reinforced with 4, 3.0 mm longitudinal bars and 1.0 mm stirrups @ 50 mm centre to centre
Roof	150 mm thick RC slab	50 mm thick RC slab
Openings D: Door W: Window	D: 1050 mm x 2700 mm W: 900 mm x 1350 mm	D: 350 mm x 900 mm W: 300 mm x 450 mm

Model SM2 was constructed to represent a typical stone masonry building used for residential purposes. These buildings consist of 375 mm thick two wythes Un-coursed Random Rubble (URR) stone masonry walls, constructed with stones placed in mud mortar and flat wooden roof with mud overlay. These buildings were the main cause of loss of life and property in the Kashmir Earthquake (Ali Q. et al., 2005).

Table 3. Model SM2 parameters

Parameter	**SM2**	
	Prototype	**Model**
Stone masonry walls	375 mm thick Un-coursed random rubble	125 mm thick Un-coursed random rubble
Stones	Undressed	Undressed
Mortar	Mud	Mud
Concrete	Concrete having compressive strength of 2.70 MPa	Concrete having compressive strength of 2.70 MPa
Reinforcement	Mild steel having yield strength of 280 MPa	Mild steel having yield strength of 280 MPa
Vertical confining elements	Only at corners; 270 mm square reinforced with 4, 10.0 mm longitudinal bars and 3.0 mm stirrups @ 150 mm centre to centre	Only at corners; 90 mm square reinforced with 4, 3.0 mm longitudinal bars and 1.0 mm stirrups @ 50 mm centre to centre

Horizontal bands	Only above openings; 150 mm thick horizontal band reinforced with 4, 10.0 mm longitudinal bars and 3.0 mm stirrups @ 150 mm centre to centre	Only above openings 50 mm thick horizontal band reinforced with 4, 3.0 mm longitudinal bars and 1.0 mm stirrups @ 50 mm centre to centre
Roof	Flexible flat wooden roof with 150 mm thick mud overlay	Flexible flat wooden roof with 50 mm thick mud overlay
Openings D: Door W: Window	D: 1050 mm x 2100 mm	D: 350 mm x 700 mm
	W: 900 mm x 1200 mm	W: 300 mm x 400 mm

It was observed during the construction of model SM2 that, unlike model SM1 where the walls were constructed with half dressed stones and cement mortar, the defect free erection of miniature scale URR walls in mud mortar was very difficult. Therefore, while constructing model SM2, vertical confining elements having very low strength concrete of around 2.7 MPa were introduced at all the four corners. Though such confining elements normally do not exist in actual buildings, they were needed in the model to avoid damage to the fragile URR walls during lifting and placing of the model on the shake table. Each wall of the model was erected in a number of lifts and concrete was poured in the confining elements incrementally after completion of each portion of wall. No continuous horizontal bands were provided in the walls. The roof was flexible, flat wooden roof with thick mud overlay, instead of RC slab. Table 3 shows the characteristics of the prototype and the scaled model SM2 and figure 4 shows the construction details of the model.

Table 4. Model SM3 parameters

Parameter	**SM3**	
	Prototype	**Model**
Stone masonry walls	375 mm thick Un-coursed random rubble	125 mm thick Un-coursed random rubble
Stones	Undressed	Undressed
Mortar	Mud	Mud

Concrete	Concrete having compressive strength of 10 MPa	Concrete having compressive strength of 10 MPa
Reinforcement	Mild steel having yield strength of 280 MPa	Mild steel having yield strength of 280 MPa
Vertical confining elements	Type 1: Only at corners; 270 mm square reinforced with 4, 10.0 mm longitudinal bars and 3.0 mm stirrups @ 150 mm centre to centre. Type 2: 75 mm x 270 mm (75 mm along the length of the wall) reinforced with 2, 10.0 mm longitudinal bars and 3.0 mm stirrups @ 150 mm centre to centre.	Type 1: Only at corners; 90 mm square reinforced with 4, 3.0 mm longitudinal bars and 1.0 mm stirrups @ 50 mm centre to centre. Type 2: 25 mm x 90 mm (25 mm along the length of the wall) reinforced with 2, 3.0 mm longitudinal bars and 1.0 mm stirrups @ 50 mm centre to centre.
Horizontal bands	At sill, lintel and roof level. 75 mm x 270 mm (75 mm along the height of the wall), reinforced with 2, 10.0 mm longitudinal bars and 3.0 mm cross-tie. @ 150 mm centre to centre.	At sill, lintel and roof level. 25 mm x 90 mm (25 mm along the height of the wall), reinforced with 2, 3.0 mm longitudinal bars and 1.0 mm cross-tie. @ 50 mm centre to centre.
Roof	Flexible Flat Wooden Roof with 150 mm thick mud overlay	Flexible Flat Wooden Roof with 50 mm inch thick mud overlay
Openings D: Door W: Window	D: 1050 mm x 2100 mm	D: 350 mm x 700 mm
	W: 900 mm x 1200 mm	W: 300 mm x 400 mm

Model SM3 was constructed by making improvements in model SM2. The objective was to investigate the extent of beneficial effect of incorporating minimal low-cost design improvements upon the earthquake resistance of stone masonry structures. Three horizontal reinforced concrete bands, each 25 mm thick (75 mm for prototype) with two longitudinal steel reinforcing bars and cross ties, at sill, lintel and roof level were introduced in the model. The width of bands in each case was equal to the width of the wall. Moreover, two types of vertical confining elements were provided in this model, which are described as follows.

Type-1 confining elements of 90 mm square (270 mm for prototype) size reinforced with four 10.0 mm longitudinal bars and closed ties, similar to the one provided in model SM2, were provided at corners. Type-2 confining elements of 25 mm x 90 mm (75 mm x 270 mm for prototype) size reinforced with two longitudinal bars and cross ties were provided around the door. Table 4 shows the characteristics of the prototype and the scaled model SM2 and figure 5 shows the construction details of the model.

SHAKE TABLE MODEL SETUP AND TESTING METHODOLOGY

The reduced scale models were tested in the Earthquake Engineering Center at the Department of Civil Engineering, University of Engineering & Technology Peshawar, Pakistan. The shaking was applied through a 1500 mm x 1500 mm one-dimensional shake table capable of applying excitation horizontally in one direction only. The models were constructed on 125 mm thick concrete pads. The model and pad assembly was then lifted and carefully mounted on the shake table and firmly secured with the help of bolts.

The North-South (N-S) component of El Centro 1940 and Kobe 1995 records were used as input excitation. In order to satisfy the similitude requirement of simple model, the time duration of the original records were compressed by a scale factor of 3. The characteristics of the original and compressed records are given in table 5.

Table 5: Characteristics of original and compressed earthquake records used in shake table tests

Input Excitation	Record	Peak Ground Acceleration, PGA (g)	Predominant Period (sec)	Excitation Duration (sec)
El Centro 1940, N-S Component	Original	0.319	0.20	30
	Compressed	0.319	0.067	10
Kobe 1995, N-S Component	Original	0.833	0.36	30
	Compressed	0.833	0.12	10

The models were subjected to ground motions by progressively increasing the amplitude of the earthquake shaking. The El Centro record was used in the initial test runs followed by Kobe

record in the final test cycles. The response of the model was captured through accelerometers and string pot displacement transducers. All gauges were connected to a data acquisition system and the data was recorded at a sampling frequency of 200 Hz. The signal data was processed for base-line correction and noise removal by employing Butterworth Band Pass Filter. Two video cameras installed at different locations were used to record damages to the walls during the test.

The model SM1 was subjected to shaking along the longer walls W1 and W3. Three accelerometers, one at the top and two at the bottom and four displacement transducers, two at the top and two at the bottom were connected to the model as shown in figure 3.

The models SM2 and SM3 were mounted on the shake table such that the direction of shaking was along one of the diagonals of the models to study both the in-plane and out-of-plane responses of the models. Two accelerometers, one at the top and other at the bottom of the models and four displacement transducers one at the bottom and three at the top were used to capture the response of the models as shown in figures 4 and 5.

SHAKE TABLE TEST RESPONSE OF THE MODELS

DYNAMIC CHARACTERISTICS

In order to determine the damping and the fundamental time period of the models, the models were subjected to a low amplitude impulse excitation before carrying out shake table tests. Damping and fundamental time period were then determined using the free vibration response of the model.

Table 6. Dynamic characteristics of stone masonry models

	SM1	SM2	SM3
Period(s)	0.07	0.08	0.09
Damping (%)	5	7	6

Table 6 gives the fundamental time periods and damping ratios of the three models, SM1, SM2 and SM3. It can be observed from the table that damping ratio and fundamental period of the three models are almost the same.

Moreover it can be seen by comparing tables 5 and 6 that predominant period of the compressed input motions and fundamental periods of the tested models are fairly close to each other. Therefore, it was expected that the input excitation would have critical Earthquake loading effect on the tested models.

OBSERVED DAMAGES AND COLLAPSE PATTERN

The cracks and resulting damages experienced by model SM1 are shown in figure 6. The figures are still images taken from one of the video cameras to capture damages to walls W1 and W4. Unfortunately the camera installed on the other side of the model to capture damages to walls W2 and W3 could not record damages due to malfunctioning of the camera. It can be seen in the figure that in the in-plane wall W1, the cracks extended diagonally between the corners of the window and corners of the wall, whereas in the out-of-plane solid wall W4, a crack at mid height emerged along the length of wall. A crack also appeared at the interface of the roof band and the walls. The cracks kept on widening with increased shaking. The propagation and widening of the cracks around the openings and at the corners of the model in the in-plane walls and the cracks at the interface of roof band and walls completely detached the out-of-plane walls from the rest of the structure. Consequently, the out-of-plane walls started vibrating like a cantilever wall resulting in their collapse, followed by collapse of the in-plane walls and ultimately resulting in collapse of the model. The overall damage pattern of the model shows that as there were no vertical and/or horizontal concrete elements except for the roof band, once the cracks initiated there was no mechanism in the model to intercept the cracks and thus the cracks propagated and widened enough to cause rapid collapse of the model. This behavior of the model indicates that though the use of cement sand mortar in stone masonry buildings may be beneficial, it alone without horizontal bands and vertical confining elements would not be sufficient for considerable improvement in the earthquake resistance of stone masonry structures.

The damages observed in the model SM2 are shown in figure 7. As the model was excited along the diagonal, all the walls were simultaneously subjected to in-plane and out-of-plane actions. In the wall W1, the diagonal cracks in the pier between the openings and the crack between the bottom corner of the window and corner of the wall are typical cracks due to in-plane mode of shaking. The out-of-plane damage to the wall W1 occurred in the form of stone falling due to disintegration of stones from the portion of the wall above the openings. The wall

W2 got damaged primarily due to out-of-plane shaking, resulting in partial collapse of the upper middle part of the wall. Damage to wall W3 initiated due to diagonal cracks on one side of the opening. However, unlike wall W1, as the lintel band was not continuous in this wall, the cracks travelled upwards and downwards towards the corners, causing further damage to the wall. These cracks coupled with out-of-plane shaking of the wall precipitated the complete collapse of the wall well before the collapse of other walls of the model. The collapse of wall W3 also caused partial collapse of the roof. The wall W4 suffered damages in the form of stone falling from upper part due to out-of-plane shaking in a manner similar to wall W2. The damage pattern of model SM2 indicates that vertical confining elements without enough horizontal bands would not be sufficient to significantly improve the earthquake resistance of such structures.

The model SM3 was also excited diagonally. The damages observed in the model SM3 are shown in figure 8. The wall W1 behaved very well to in-plane shaking, however, as the vertical elements around the door were curtailed at the lintel level and were not extended up to the roof of the model, the wall above the lintel level collapsed in an out-of-plane direction. The out- of-plane shaking also caused dislodging and falling of stones from the upper portion of wall W2. Wall W3 did not get damaged except for an apparent sliding at the interface of lintel band. Some stones fell down from upper portion of wall W4 in a manner similar to wall W2. Apart from these observed damages, unlike models SM1 and SM2, model SM3 did not undergo complete collapse and survived the earthquake excitation. The performance of SM3 model is therefore considered to be much better that that of models SM1 and SM2. The incorporation of vertical RC elements and RC horizontal bands helped improving the structural response of the model. In addition to introducing box-like structural behavior in the model, these elements also divided the walls into small portions resulting in more resistance to out-of-plane collapse. The smaller these wall portions are, the less the damage they will experience. Furthermore, the damage pattern of the model indicates that the distance between the vertical confining elements is also important for preventing out-of-plane collapse of walls.

SEISMIC CAPACITY IN THE FORM OF BASE SHEAR COEFFICIENT vs. DRIFT RATIO

The data obtained during shake table test was processed and the results obtained were converted to prototype response according to the similitude requirements of table 1. The input and response acceleration values were multiplied by 0.33 to obtain the prototype values.

Therefore all values mentioned hereinafter pertain to the relevant prototypes of the models. Moreover as models SM2 and SM3 were subjected to shaking along one of the diagonals, the net resultant response of models SM2 and SM3 along the diagonal was resolved into two components to obtain the relevant in-plane response along walls W1 and W3.

The prototype capacity curve of all three models in the form of Base Shear Coefficient (BSC) vs. drift ratio is presented in fig 9. Drift ratio is the ratio of top lateral displacement to height of the model and is expressed as percent drift. The BSC is determined as the ratio of base shear to the total weight of model. Base shear is calculated by multiplying the maximum response acceleration at the story level with the storey mass; storey mass being taken equal to sum of the mass of roof and half of the mass of walls.

The advantage of comparing capacity in the form of BSC instead of Peak Ground Acceleration (PGA) is that it provides a uniform standard for comparing performance of structures subjected to varied testing regimes, and thus similar structures tested anywhere in the world can be conveniently compared without giving specific importance to input excitation and PGA. As BSC is a function of response acceleration which is further a product of amplification factor and PGA, the BSC will depend on the product of amplification factor and PGA. The value of amplification factor depends on how closely the frequency of input excitation matches with the frequency of the model. In the case of a close match, there will be good amplification producing higher response acceleration and damaging the model at less PGA. In other case if there is less amplification due to poor match, the model will keep on taking higher PGA to produce similar degree of damage. However as BSC depends on the product of amplification factor and PGA, the BSC in both cases would be almost the same.

Figure 9 compares the responses of models SM1 and SM2 to SM3 in terms of BSC versus drift. It can be seen that seismic resistance of model SM3 is much higher than those of models SM1 and SM2 and that BSC of models SM1 and SM2 corresponding to various drift ratios is almost similar. It can also be seen that BSC of all models is nearly equal up to a drift ratio of 0.07 % indicating that the models have suffered no or very minor damages during this stage with no substantial reduction in their stiffness. However, afterwards from 0.07 to 0.6 % drift ratios, the BSC corresponding to same drift ratio for model SM3 is much higher than those of models SM1 and SM2 indicating that models SM1 and SM2 have experienced moderate to major

damages during this stage resulting in sharp stiffness degradation. The models SM1 and SM2 have reached their peak capacity at drift ratio of around 0.6 % corresponding to BSC of 0.17 whereas model SM3 reached its peak capacity at drift ratio of 0.78 % corresponding to BSC of 0.28. It is worth mentioning that the values of drift ratios reported here do not necessarily include the drifts obtained from structural displacement only but they may also contain some localized vibration effects mainly due to rocking of walls, especially at test runs close to failure.

The amplification factors for the models determined from the test data are reported in figure 10 which shows that amplification factor decreases with increase in drift ratio. The reason for this trend is very obvious. Initially the models were having low periods closely matching with the dominating period of the input motions. However the period of the models increased with decrease in stiffness after the models suffered damages resulting in relatively less match and low amplification factors. For practical range of drift ratios, however, an average value of 1.6 is reported.

DAMAGE LIMIT STATES AND ELASTO-PLASTIC IDEALIZATION

Keeping in consideration the observed damages and capacity curves given in figure 9, damage limit states for the prototypes of all models are recommended in table 7. The table shows that drift ratios and BSC corresponding to all three damage limit states for models SM1 and SM2 are nearly equal whereas these values are around half of those reported in the same range for model SM3.

As already mentioned, there was a major difference between the damage pattern of model SM1 and models SM2 and SM3. In the model SM1, the cracks appeared around openings, at corners and at interface of RC roof band and walls, which then ultimately caused the collapse of the model similar to any brick or block masonry structure with masonry units placed in cement sand mortar and RC roof. In the models SM2 and SM3, as the walls consisted of random-ruble masonry placed in mud mortar, the collapse in the form of stones dislodging and falling from upper parts of the out-of-plane walls due to inadequate bond between stones was the main cause of damage. The damage limit states in the model SM1 are therefore governed by initiation and widening of cracks leading to total collapse of structure, whereas they are mainly governed by out-of-plane collapse of walls in the form of stone falling in the models SM2 and SM3.

Figure 11 shows the elasto-plastic idealized curves of the models. The curves were derived from equal energy principle (Magenes and Calvi 1997) with modification in the ultimate drift ratio based on visual observation of the tests. According to the equal energy principle, the yield strength is taken as 90% of the measured peak strength. The ultimate drift is taken as the point where the yield strength degrades by 20 % or measured peak strength degrades by 28 %. The ultimate drift found by this approach was found to be too high as compared to the actual degradation in the peak strength noticed from the visual observation of damages. Therefore the point of ultimate drift was fixed from observed damages in the models. Such a point in each case was however found to fall in the vicinity of the point of intersection of the lines joining the flat portion of elasto-plastic curve and the descending branch of experimental curve. Consequently, drift ratio corresponding to this intersection point was taken as the ultimate drift for all elasto-plastic curves.

Table 7: Drift ratio (%) and BSC corresponding to different damage levels

Model	**Parameters**	**Damage Levels**		
		Immediate Occupancy	**Life Safety**	**Collapse Prevention**
SM1	Drift Ratio (%)	0.15	0.4	0.6
	BSC	0.06	0.1	0.17
	Damage Condition	Stage just prior to minor cracks in walls.	Minor to moderate cracks in walls and at the interface of roof and walls.	Further widening of cracks. Stage prior to collapse.
SM2	Drift Ratio (%)	0.1	0.3	0.6
	BSC	0.05	0.1	0.17
	Damage Condition	Stage just prior to initiation of stone falling.	Initiation of stone falling and minor to moderate damage to walls.	Further stone falling and stage prior to partial collapse of roof
SM3	Drift Ratio (%)	0.25	0.6	1.3
	BSC	0.1	0.2	0.28
	Damage Condition	Stage just prior to initiation of stone falling.	Initiation of stone falling and minor to moderate damage to walls.	More damage to walls by stone falling. Roof and RC elements remained intact

RESPONSE MODIFICATION FACTOR "R"

Two different techniques have been used to compute R for the models in order to take care of the inherent uncertainties in the definition of R. The first approach is based on the energy-balance criterion using the classical analytical model, as given in equation 1.

$$R = \sqrt{2\mu - 1} \text{ where } \mu = \frac{d_u}{d_y} \quad (1)$$

Where μ represents the displacement ductility, d_u represents the ultimate displacement capacity and d_y represents the yield displacement. The energy-balance criterion is used due to the fact that the fundamental time period of the prototype of tested models lies on the constant acceleration part of the design spectra of Building Code of Pakistan, Seismic Provision (BCP S-P2007, adopted mostly from UBC-97). The same approach has been used also by other researchers (Tomazevic and Weiss, 2010).

The second approach, as given in equation 2, is based on incremental dynamic analysis (IDA) of inelastic structure following the early proposal of Kappos (Kappos 1991), recommended and employed elsewhere (Elnashai and Broderick, 1996; Mwafy and Elnashai, 2002) and which is also used recently (Ali *et al*., 2012; Zafar and Andrews, 2011;).

$$R = \frac{PGA_u}{PGA_y} \quad (2)$$

PGA_u represents the target PGA of ground motions causing the collapse of structure and PGA_y represents the target PGA causing the yielding of the structure.

A single degree of freedom (SDOF) system is designed with similar stiffness and strength for case study structures. Seismic masses are then assigned to the model in order to simulate the fundamental vibration period of structures. A nonlinear Takeda type rule (Otani, 1974), with unloading stiffness as proposed by Emori, K., and Schnobrich (Emori, K., and Schnobrich, 1978) , is used for IDA which is also used elsewhere for nonlinear dynamic time history analysis (Ahmad *et al*., 2010, Menon and Magenes, 2011).

A suit of ten natural accelerograms are employed, compatible to the BCP (2007) elastic design spectrum for stiff soil (Type D of NEHRP classification). A demand chart was developed between different target PGA and ductility demand which was then interpolated to compute PGA at yielding and ultimate limit states of the models, figure 12. The characteristics demand chart i.e. the 16th percentile value which has 84 percent chances of exceedance, is used to compute R. The values of R resulting from these approaches are given in table 8, which shows that an average estimate of 1.5 may be used for models SM1 and SM2 and a value of 2.0 may be used for model SM3.

Table 8. Response Modification Factors

Structure Type	Methodology		
	Equal Energy	IDA	Recommended
SM1	1.91	1.87	1.5
SM2	1.70	1.61	1.5
SM3	2.49	2.36	2.0

USE OF STONE MASONRY BUILDINGS IN VARIOUS SEISMIC ZONES

According to the Building Code of Pakistan, Seismic Provision (BCP SP-2007), the base shear for low period structures can be calculated using equation 3 (equation 5-30.5 of BCP-SP2007, equation 30.5 chapter 16 of UBC-97) as follows:

$$V = BSC \times W \tag{3}$$

$$BSC = (2.5\ C_a\ I/R) \tag{4}$$

W = Weight of the structure

C_a = Seismic coefficient depending on seismic zone

I = Importance factor

R = Response modification factor

The current version of BCP SP-2007 recommends that buildings be designed for ultimate or collapse prevention level based on seismic demand corresponding to the seismic zone where the building is located. The C_a values for different seismic zones in the order of increasing seismic

demand from zone 1 to 4 with zone 1 as the low seismic zone and zone 4 as the most severe seismic zone are given in table 5.17 of BCP SP-2007 (table 16-Q, chapter 16 of UBC-97. Therefore taking relevant C_a values, importance factor "I" equal to 1.0, and R equal to 2.0 for model SM3 and 1.5 for models SM1 and SM2 as determined in the previous section, the resulting demand BSCs corresponding to each seismic zone for the models are given in table 9. The collapse level experimental Base Shear Coefficient (BSC_E) as reported in table 7 are reproduced in table 9 to determine the use of these structures in various seismic zones corresponding to ultimate or collapse prevention level. The data presented in table 9 indicates that typical SM1 and SM2 stone masonry structures can be recommended for use in zones 1 and 2a but not in the higher seismic zones. Similarly stone masonry buildings constructed according to SM3 characteristics can be recommended for use in zones 1, 2a, 2b and 3.

Table 9. Seismic performance of stone masonry structures in various seismic zones

			SM1 & SM2			**SM3**		
Zones	**Level of seismic hazard**	**C_a**	**Demand BSC = $2.5C_aI/R$ (R = 1.5)**	**BSC_E**	**Seismic Performance**	**Demand BSC = $2.5C_aI/R$ (R = 2.0)**	**BSC_E**	**Seismic Performance**
1	Low	0.06	0.10	0.17	OK	0.08	0.28	OK
2A	Lower moderate	0.12	0.20		OK	0.15		OK
2B	Upper moderate	0.16	0.27		NG	0.20		OK
3	High	0.24	0.40		NG	0.30		OK
4	Very high	0.32	0.53		NG	0.40		NG

CONCLUSIONS AND RECOMMENDATIONS

- The performance comparison of models SM1 and SM3 indicates that although the use of cement sand mortar in stone masonry buildings may be beneficial, it alone without horizontal bands and vertical confining elements would not be sufficient for substantial improvement in the seismic capacity of stone masonry structures.
- The performance comparison of models SM2 and SM3 indicates that vertical RC elements placed only at corners without horizontal bands would not appreciably improve the seismic performance of stone masonry structures.

- The damping ratio of stone masonry structures do not significantly vary with type of masonry construction and it can be approximately taken as 5 % for almost all types of stone masonry structures.
- The horizontal bands at the sill, lintel and roof level substantially enhance the capacity of the structure by introducing box effect in the structure.
- More number of horizontal bands even though if they are as thin as 75 mm are proved to be more efficient than single thick horizontal band, e.g. 75 mm thick horizontal bands provided at sill, lintel and roof level will enhance the capacity of the structure much more than single 150 mm thick lintel or roof band.
- SM1 and SM2 type stone masonry structures can be used in zones 1 and 2a but cannot be used in zones 2b, 3 and 4.
- SM3 type stone masonry structures can be used in zones 1, 2a, 2b and 3.
- The details of horizontal band and vertical confining elements to be provided in SM3 type stone masonry structures are given as follows:
    a. Horizontal bands: 75 mm x 270 mm (75 mm along the height of the wall), reinforced with 2, 10.0 mm longitudinal bars and 3.0 mm cross-tie. @ 150 mm center to center. These bands shall be provided at sill, lintel and roof level.
    b. Vertical confining elements:
        i. Type 1 confining element: 270 mm square reinforced with 4, 10.0 mm longitudinal bars and 3.0 mm stirrups @ 150 mm center to center.
        ii. Type 2 confining element: 75 mm x 270 mm (75 mm along the length of the wall) reinforced with 2, 10.0 mm longitudinal bars and 3.0 mm stirrups @ 150 mm center to center.

ACKNOWLEDGEMENTS

The authors greatly acknowledge the financial support from the Board of Advanced Studies and Research at Khyber-Pakhtunkhwa University of Engineering & Technology Peshawar, Pakistan and the Higher Education Commission (HEC) Islamabad. The authors also acknowledge the support of lab staff, especially Mr. Khan Zamir of Earthquake Engineering Center at University of Engineering & Technology Peshawar.

REFERENCES

Ahmad, N., Crowley, H., Pinho, R. and Ali, Q., 2010. Displacement-based earthquake loss assessment of masonry buildings in Mansehra city, Pakistan. *Journal of Earthquake Engineering*, 2010;Vol. 14, No. S1, pp. 1-37.

Ali, Q., Schacher, T., Ashraf, M., Alam, B., Naeem, A., Ahmad, N. and Umar, M., 2012. In-plane behavior of Dhajji-Dewari structural system (wooden braced frame with masonry infill), *Earthquake Spectra, Journal of Earthquake Engineering Research Institute*. Accepted for publications.

Ali. Q et al., 2005, First Report on the Kashmir Earthquake of October 08, 2005, Learning from Earthquakes, *Earthquake Engineering Research Institute USA special reports*.

Ali Q, Mohammad T., 2006, Stone masonry residential buildings in northern areas of Pakistan, *World Housing Encyclopedia*, EERI. www.eeri.org

Ali Q and Naeem A., 2007, Seismic resistance evaluation of unreinforced masonry buildings, *Journal of Earthquake Engineering*, (11 no.2),133-146.

Asian development bank and World Bank, 2005, Preliminary damage and needs assessment, *Pakistan 2005 earthquake*, web.world.bank.org.

Calvi, G.M., Kingsley, G.R., Magenes, G., 1996, Testing masonry structures for seismic assessment, *Earthquake Spectra, Journal of Earthquake Engineering Research Institute*, 12 (1), 145-162.

EERI, World Housing Encyclopedia, 2008, Tutorial on stone masonry buildings, *Earthquake Engineering Research Institute, USA*, www.eeri.org.

Elnashai, A. S. and Broderick, B. M., 1996. Seismic response of composite frames - II. Calculation of behaviour factors, *Engineering Structures*, Vol. l8, No. 9, pp. 707–723.

Emori, K., and Schnobrich, W.C., 1978. Analysis of reinforced concrete frame-wall structures for strong motion earthquakes, *Structural Research Series No. 434*, Civil Engineering Studies, University of Illinois at Urbana-Champaign, USA.

Gulkan, P. et al., 1979, Shaking Table Study of Single-Story House-Volume 2: Test structures 3 and 4, *Earthquake Engineering Research center*, Report No.UCB/EERC-79/24.

G. Vasconcelos1 et al., 2006, Experimental Investigations on Dry Stone Masonry Walls, *1st International Conference on Restoration of Heritage Masonry Structures* Cairo, Egypt April 24-27

IAEE, 1986, Guidelines for Earthquake Resistant Non-Engineered Construction, *International Association for Earthquake Engineering, Tokyo*, available on www.nicee.org.

IS 13828, 1993, Indian Standard Guidelines for Improving Earthquake Resistance of Low-strength Masonry Buildings, *Bureau of Indian Standards, New Delhi.*

Kappos, A.J. 1991, Analytical prediction of the collapse earthquake for reinforced concrete buildings: suggested methodology, *Earthquake Engineering & Structural Dynamics*, Vol. 20, No. 2, pp. 167-176.

Magenes G and Calvi M. 1997, In-Plane Seismic Response of Brick Masonry Walls, *Earthquake Engineering and Structural Dynamics*, Vol. 26, 1091-1112.

Menon, A., and Magenes, G., 2011, Definition of seismic input for out-of-plane response of masonry walls, *Journal of Earthquake Engineering*, 2011, Vol. 15, No. 2, pp. 165-194.

Mann, W., Muller, H., 1982, Failure of Shear Stressed Masonry - An Enlarged Theory, Tests and Application to Shear Walls, *The Structural Engineer, Proc. British Ceramic Society*, 30, 223-235.

Naseer, A., Naeem, A., Hussain, Z. and Ali, Q. 2010. Observed seismic behavior of buildings in northern Pakistan during the 2005 Kashmir earthquake. Earthquake Spectra, Vol. 26, No. 2, 425-449.

Otani, S., (1974). SAKE, a computer program for inelastic response of R/C frames to earthquakes, *Report UILU-Eng-74-2029*, Civil Engineering Studies, University of Illinois at Urbana-Champaign, USA.

Tomazevic, M., 1999, Earthquake Resistant Design of Masonry Buildings, *Imperial College Press, London.*

Tomazevic, M., and Weiss, P., 2010, Displacement capacity of masonry buildings as a basis for the assessment of behavior factor: an experimental study, *Bulletin of Earthquake Engineering*, Vol. 8, No. 6, pp.1267-1294.

Mwafy, A. M. and Elnashai, A. S., 2002, Calibration of force reduction factors of reinforced concrete buildings, *Journal of Earthquake Engineering*, Vol. 6, No. 2, pp. 239–273.

Zafar, A., and Andrawes, B., 2011, Response modification factor for reinforced concrete buildings in Pakistan, *Proceedings of the International Conference on Earthquake Engineering and Seismology;* Islamabad, Pakistan.

List of tables	
Table no.	Caption
1	Similitude requirement for simple model
2	Model SM1 parameters
3	Model SM2 parameters
4	Model SM3 parameters
5	Characteristics of original and compressed earthquake records used in shake table tests
6	Dynamic characteristics of stone masonry models
7	Drift ratio (%) and BSC corresponding to different damage levels
8	Response Modification Factors
9	Seismic performance levels of the stone masonry structures in various seismic zones

List of figures	
Figure no.	Caption
1	Typical Stone masonry building with two Wythes, (b) Two wythe coursed random rubble-stone masonry with half dressed stones, (c) Two wythe random rubble-stone masonry wall
2	Use of horizontal and vertical timber elements in stone masonry building
3	Reduced scale model SM1 and its instrumentation detail for shake table test
4	Reduced scale model SM2 and its instrumentation detail for shake table test
5	Reduced scale model SM3 and its instrumentation detail for shake
6	Damages observed in model SM-1
7	Damages observed in model SM-2
8	Damages observed in model SM-3
9	BSC vs. Drift ratio (%) curves of the prototype of each model
10	Variation of amplification factors with drift ratio.
11	Idealized elasto-plastic curves.
12	Drift demand on stone masonry structures through IDA (a) SM1, (b) SM2, and (c) SM3.

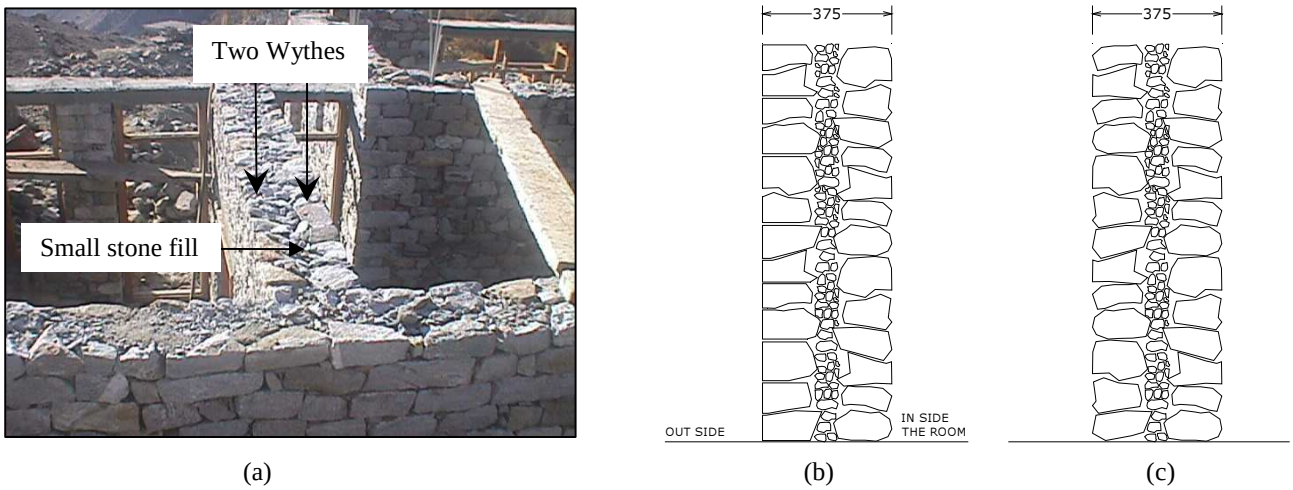

Figure 1. (a) Typical Stone masonry building with two Wythes, (b) Two wythe coursed random rubble-stone masonry with half dressed stones, (c) Two wythe random rubble-stone masonry wall

Figure 2. Use of horizontal and vertical timber elements in stone masonry building.

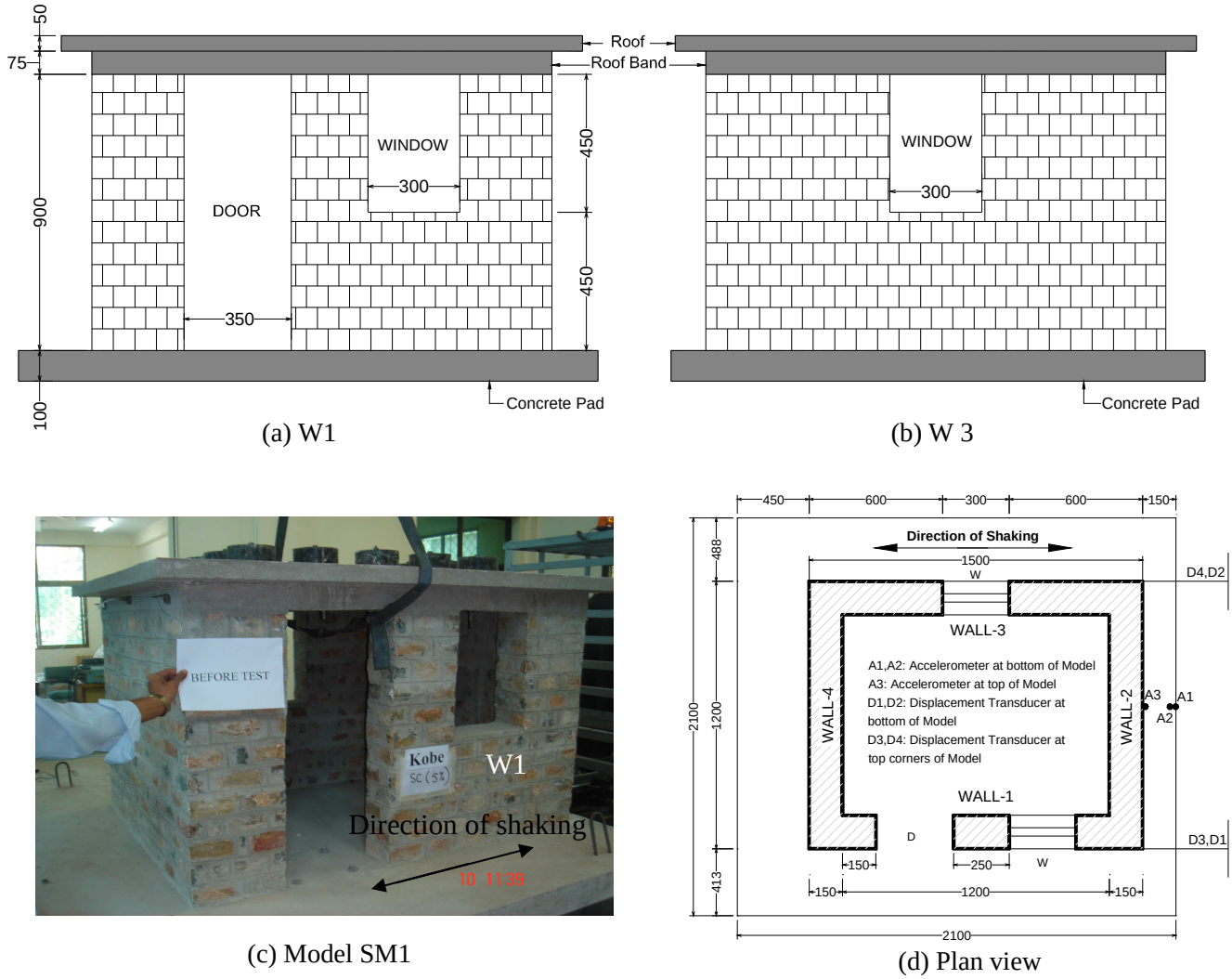

(a) W1 (b) W 3

(c) Model SM1 (d) Plan view

Figure 3. Reduced scale model SM1 and its instrumentation detail for shake table test.

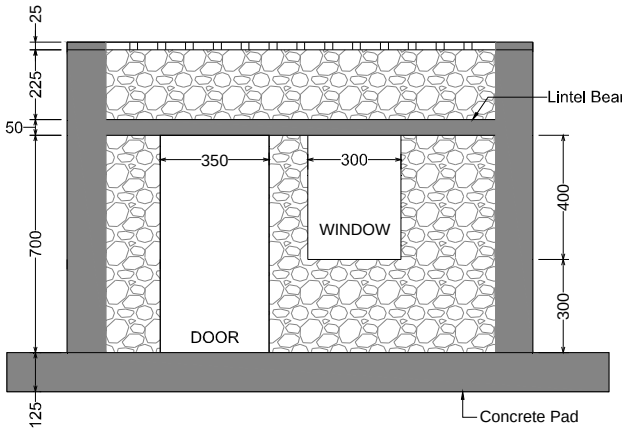

(a)W1

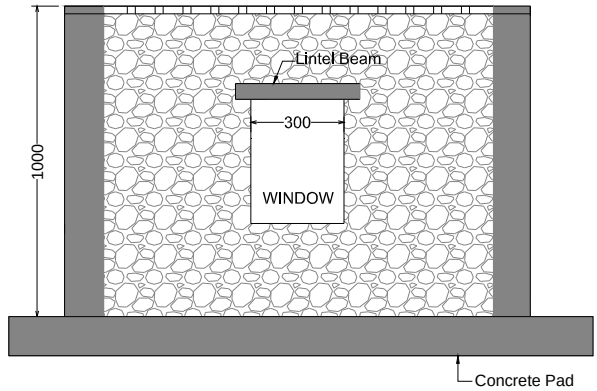

(b) W3

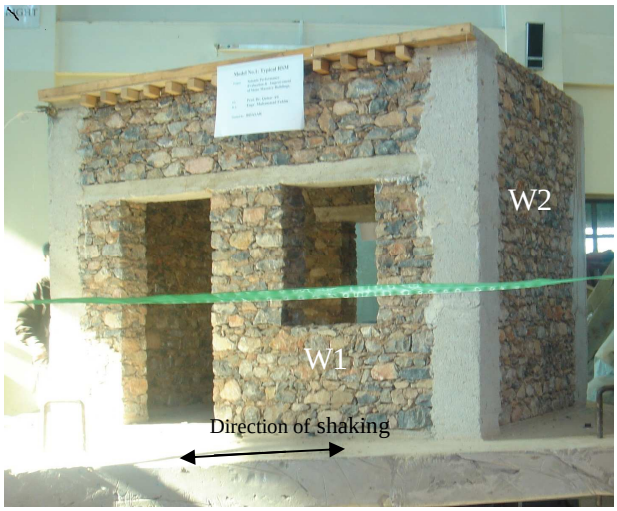

(c) SM2 Model

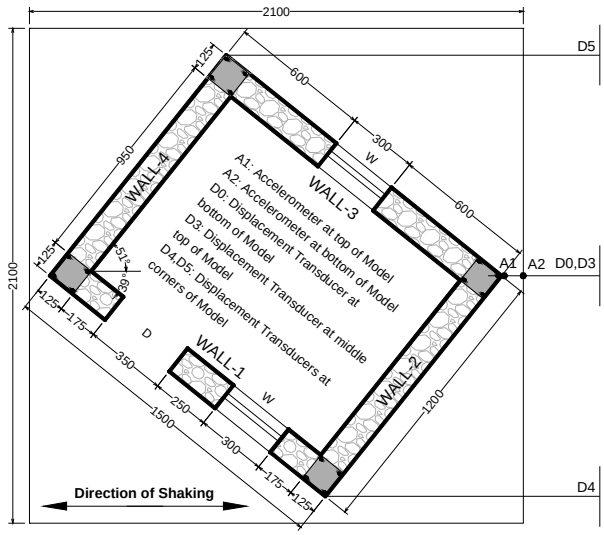

(d) Plan

Figure 4. Reduced scale model SM2 and its instrumentation detail for shake table test.

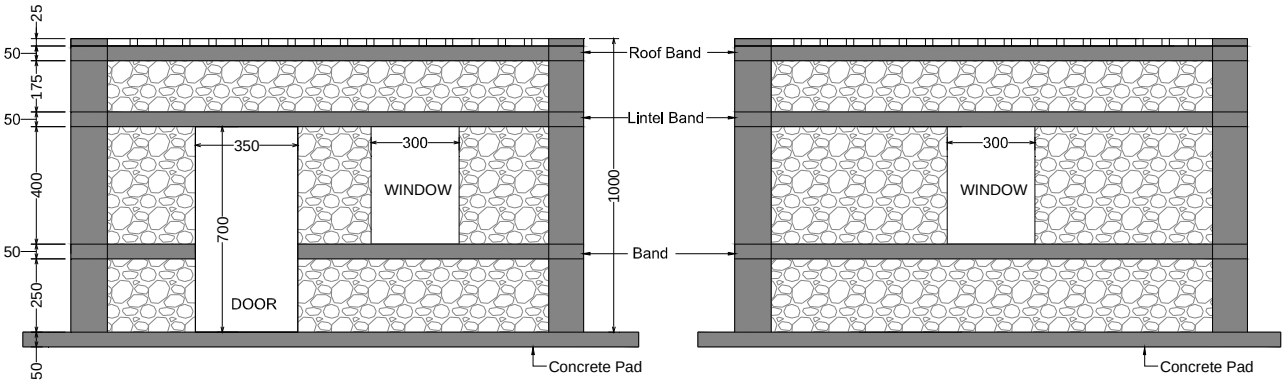

(a) W1 (b) W3

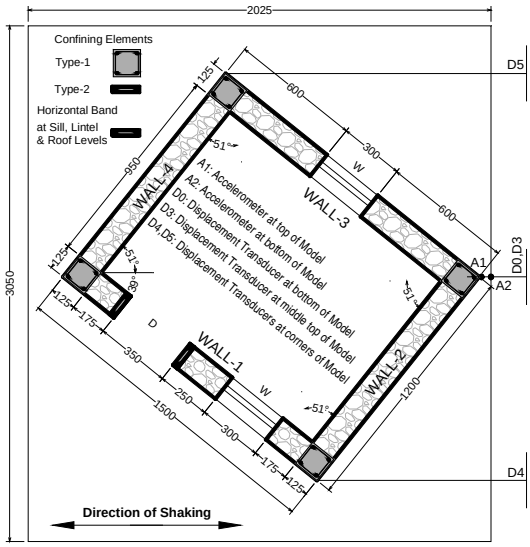

(c) Model SM3 (d) Plan

Figure 5. Reduced scale model SM3 and its instrumentation detail for shake table test

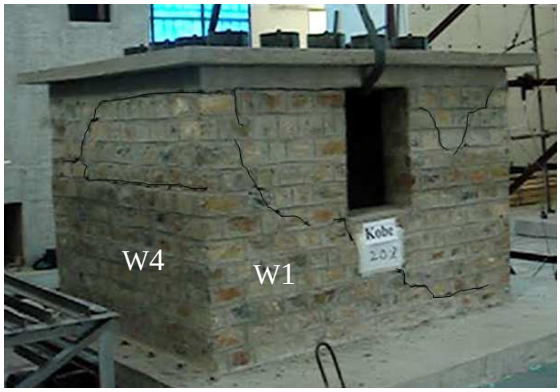

(a) Initiation of diagonal and longitudinal cracks in W1 and W4

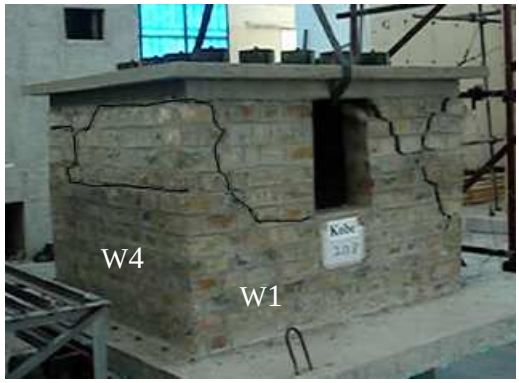

(b) Widening of diagonal and longitudinal cracks in W1 and W4

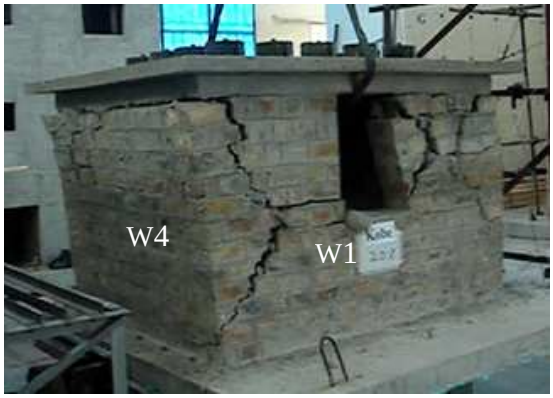

(c) Initiation of collapse

(d) Collapse of model

Figure 6. Damages and collapse of model SM1

(a) Initiation of cracks in W1

(b) Widening of cracks in W1

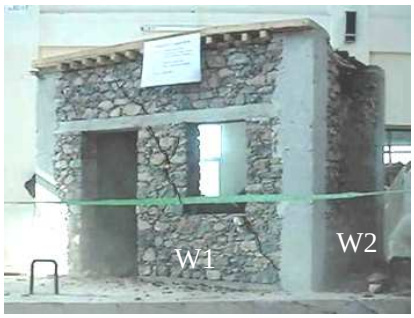

(c) Further widening of cracks in W1 and initiation of out-of-plane collapse of W2

(d) Further widening of cracks in W1 and partial collapse of W2

(e) Initiation of cracks in W3

(f) Widening of cracks in W3

(g) Initiation of collapse of W3

(h) Collapse of W3 and damage to W4

Figure 7. Damages and collapse of model SM2

(a) Initiation of diagonal cracks in W1 and stone falling from W2

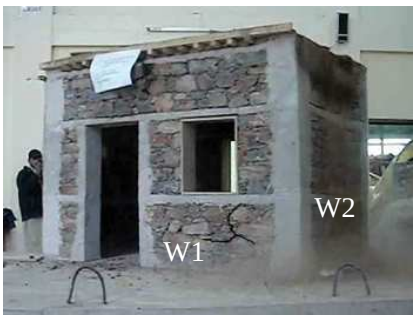

(b) Widening of diagonal cracks in W1 and stone falling from W2

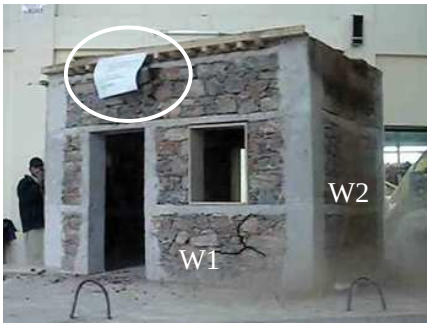

(c) Initiation of out-of-plane collapse of W1

(d) Partial out-of-plane Collapse of W1

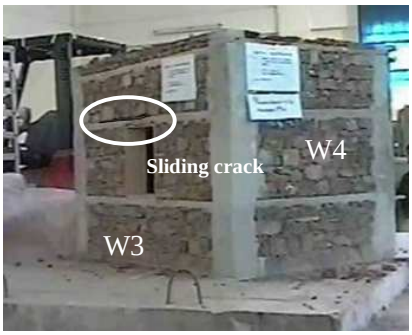

(e) Initiation of sliding crack in W3

(f) Widening of sliding crack W3 and minor stone falling from W 4

Figure 8. Damages observed in model SM3

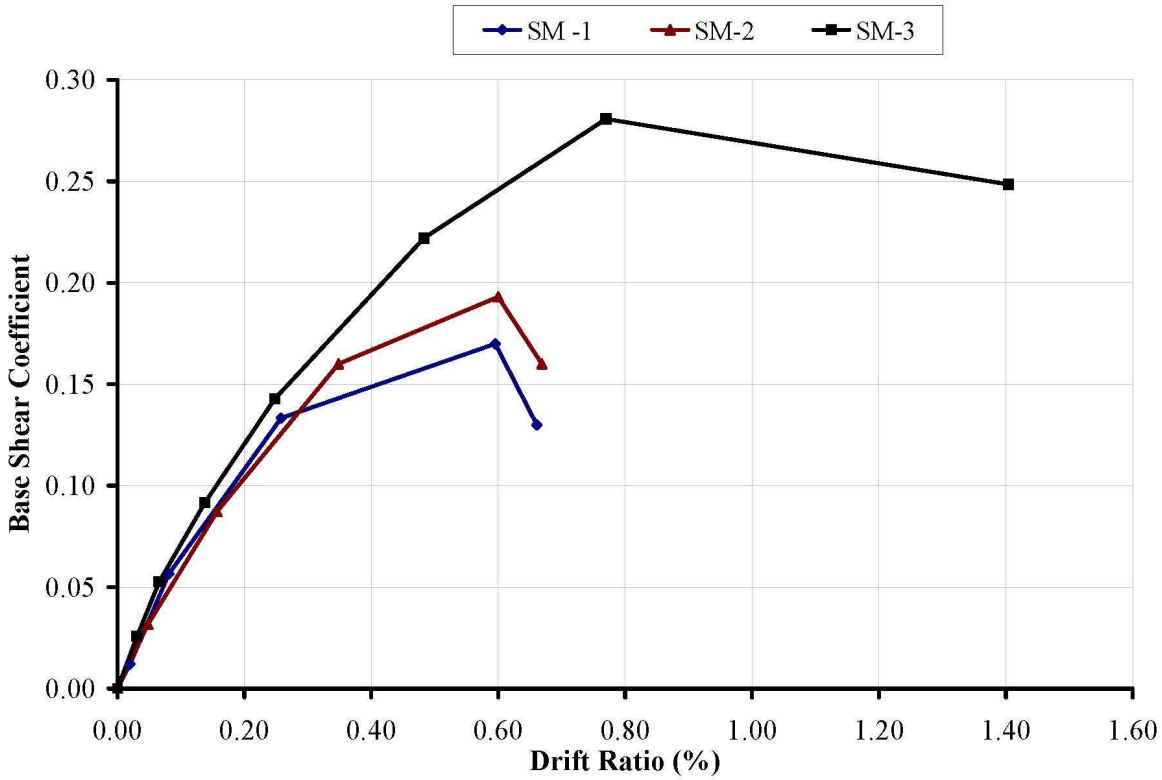

Figure 9. BSC vs. Drift ratio (%) curves of the prototype of each model

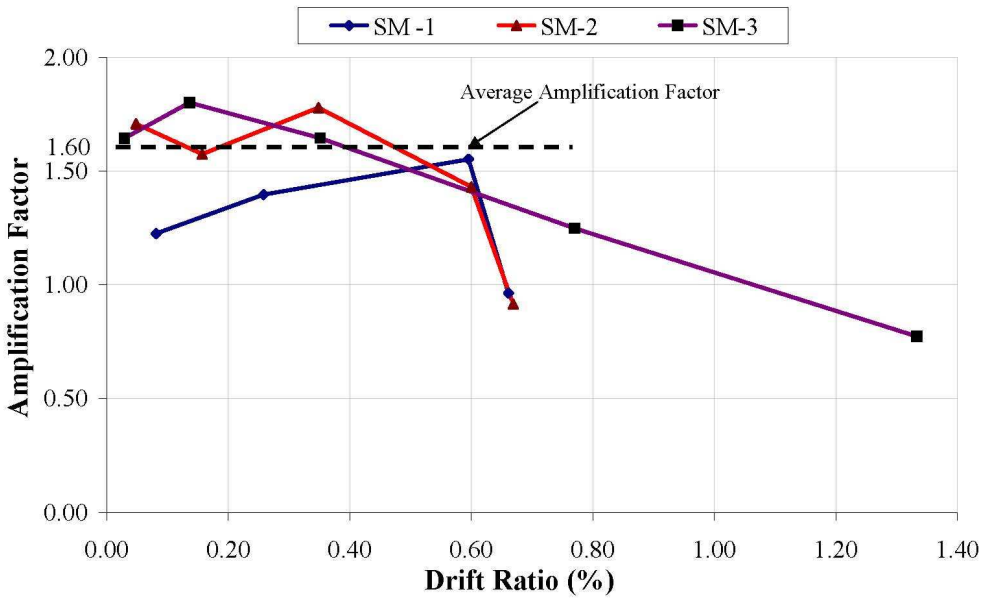

Figure 10. Variation of amplification factors with drift ratio.

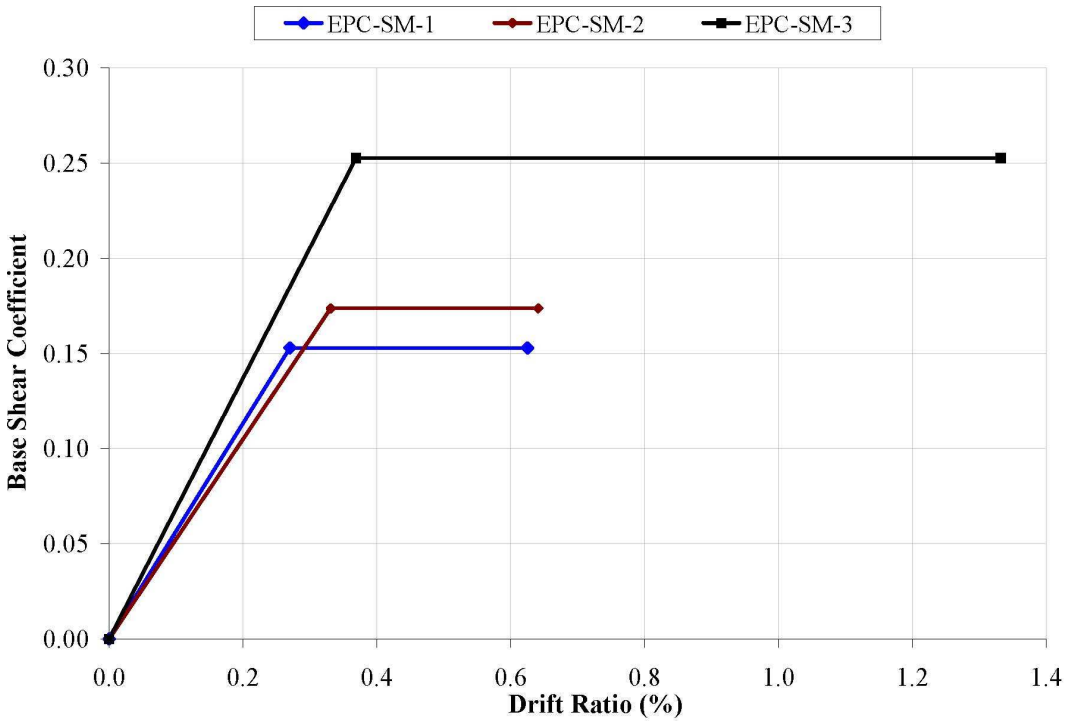

Figure 11. Idealized elasto-plastic curves.

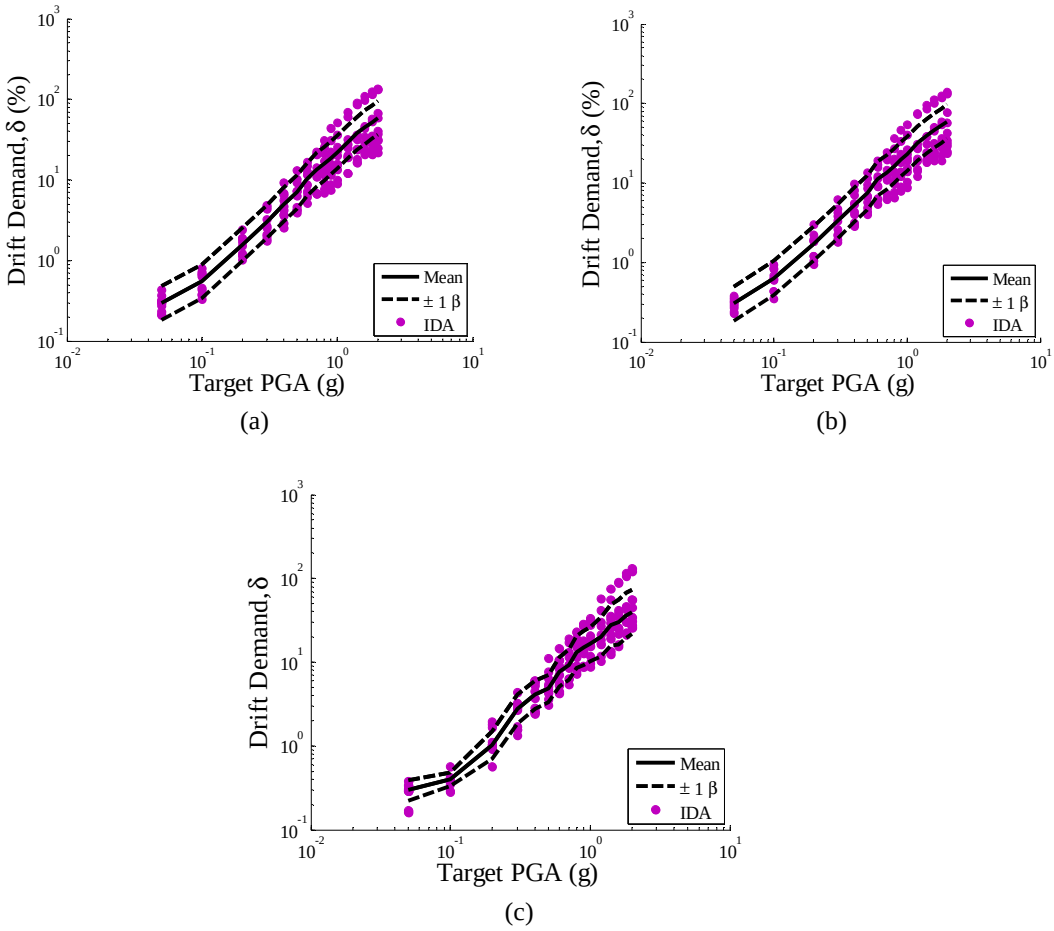

Figure 12: Drift demand on stone masonry structures through IDA. *From top to bottom and left to right:* SM1, SM2, and SM3.

Appendix

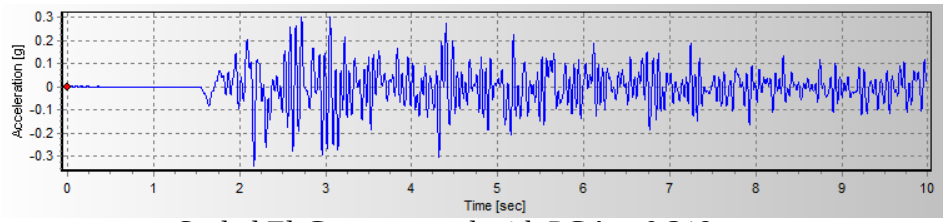

Scaled El-Centro record with PGA = 0.319g

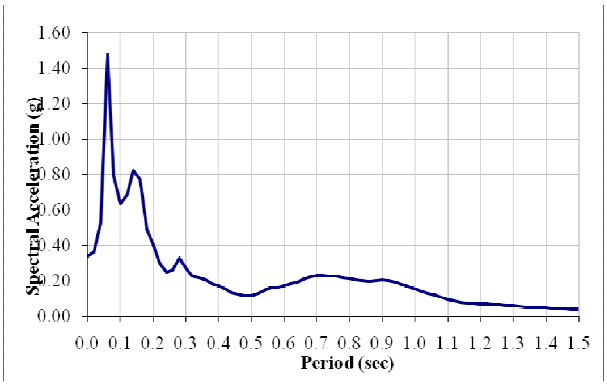

Response Spectrum of El-Centro compressed record.

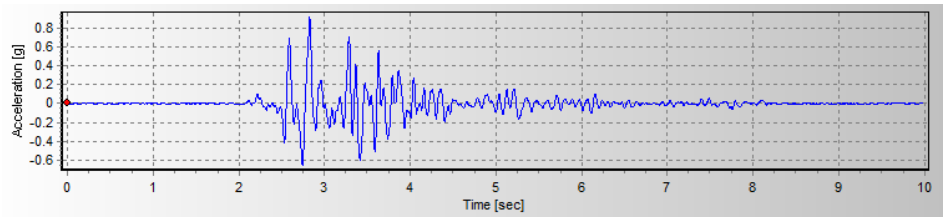

Scaled Kobe record with PGA = 0.833g

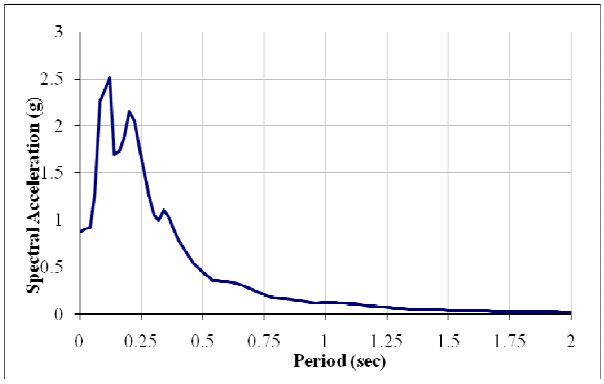

Response Spectrum of Kobe compressed record.